Chaos at moderate eccentricities for the 2:1 resonant asteroid motion.

George Voyatzis
Section of Astrophysics, Astronomy and Mechanics
Department of Physics, University of Thessaloniki,
54006 Thessaloniki, Greece

Abstract

The formation of the Hecuba gap close to the 2:1 resonant asteroid mean motion with Jupiter is examined. We consider a symplectic mapping model and its phase space dynamics is studied by using spectral maps. It is shown that fast diffusion is possible even inside the region of moderate eccentricities (0.2 - 0.5) and low inclinations where previous studies indicate islands with ordered motion.

1 The Model

In the last decades, the explanation of the Kirkwood gaps is studied within the framework of the restricted 3 (or 4) body problem and it is traced back to the existence of chaotic motion. The reader can find more details about the topic of resonant asteroid dynamics in [1, 2]. Since the numerical integration of the equations of the original system are cpu-time consuming, generally, approximations of the models are used in order to study the long term evolution of asteroids. Our model is constructed by considering the following approximations:

Averaging [3] The Hamiltonian of the original system, is written as a perturbed two body problem, i.e. $H = H_0 + R$, where R is the perturbation or disturbing function. R is expanded as a multiple Fourier transform and, by introducing suitable resonant variables $(\lambda, \sigma, \nu, \sigma_z, \Lambda, S, N, S_z)$, and averaging in respect to the fast angle λ (mean longitude), we get the averaged Hamiltonian $\hat{H}(\sigma, \nu, \sigma_z, S, N, S_z)$.

Symplectic map [4] Let the index $n = 1, 2, ...,$ denotes the values of the phase space variables at time $t = nT$, where T is the period of Jupiter. Then a symplectic map is constructed by considering the generating function

$$W = S_{n+1}\sigma_n + N_{n+1}\nu_n + Sz_{n+1}\sigma_{zn} + T \cdot \hat{H}'(S_{n+1}, \sigma_n, N_{n+1}, \nu_n, Sz_{n+1}, \sigma_{zn})$$

where $\hat{H}' = \hat{H} + H_{cor}$ and H_{cor} enters corrections such that the periodic orbits of the original system fit in with the fixed points of the mapping in respect to location and stability. The detailed form of the mapping is given in [5].

2 Spectral Maps

We can explore large subsets of the phase space and determine whether chaos or order is apparent by applying the spectral method, introduced in [6]. According to this method we calculate a trajectory and we consider the variation of a slow variable $X(t)$. Then, the power spectral density, $P(f)$, of the series $X_1, X_2, ..., X_N$ is calculated. When an invariant torus is simply deformed after a perturbation (i.e. torus preserves its topology and is twisted by quasiperiodic orbits) the power included in the low frequencies of the $P(f)$ converges exponentially. When the invariant torus breaks up, giving rise to chaotic motion, the low frequency domain shows an irregular continuous distribution of the low frequency spectral peaks that possesses a relatively significant power. Conclusively, the classification of the

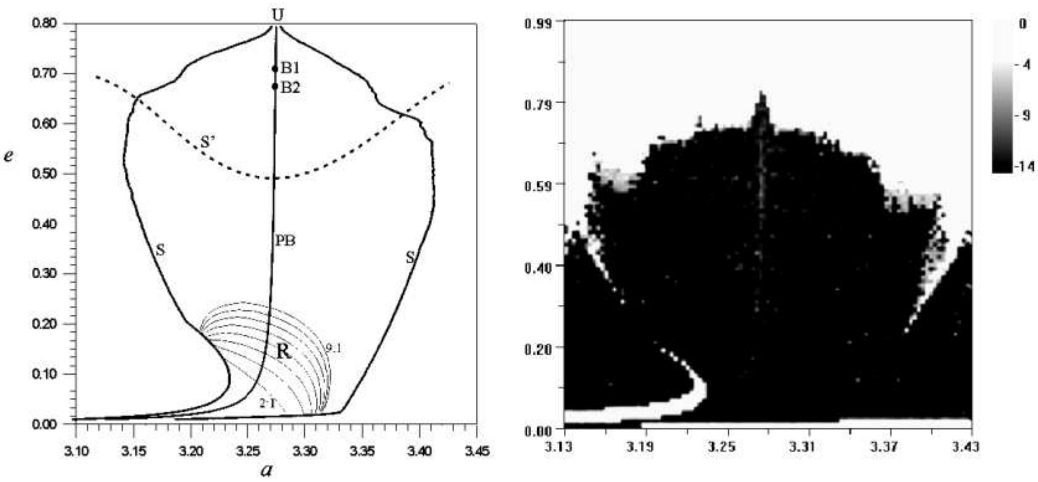

Figure 1: (left) The dominant phase space characteristics for $\sigma = 0$ on the plane $a - e$ (right) chaotic (light) and ordered regions (dark) for the circular problem observed by using spectral analysis

trajectories, as regular or chaotic, can be based on the low frequency band of the power spectrum or , practically, on the power included in the $k(<< N/2)$ lowest available spectral lines. In practice the following estimator is used

$$\beta_k = \log_{10}(\bar{P}_k/\bar{P}_{N/2}) \qquad , \qquad \bar{P}_m = \sum_{i=1}^{m} P(f_i) \tag{1}$$

Generally, for regular orbits is $\beta_k < -10$ while, for chaotic orbits, β_k is usually found greater than -5 (note the logarithmic scale).

In the following , we consider grids of size about 100×100) of initial conditions on the (a, e) planes (semimajor axis, eccentricity), for fixed values $\sigma = \nu = \sigma_z = 0$ and inclination i=const. For each point on the grid, we calculate the corresponding trajectory for $N = 131072$ iterations (about 1.5 Myr), we apply Hanning Filter and FFT and we calculate the estimator $\beta = \beta_4$. The β-levels are mapped to a gray palette. Dark scales refer to small values of β (order), while the light ones refer to relatively large values of β (chaos). The Jupiter's eccentricity (e') and inclination (i') are parameters, which are set both to zero for the circular-planar case, $e' = 0.048$ and $i' = 0$ for the elliptic-planar case and also is $i' = 1^o$ for any spatial case.

3 Dominant characteristics of the 2:1 resonant dynamics

The dominant characteristics of the phase space are formed by the fixed points of our model and the corresponding separatrices of the unstable fixed points. For the Circular case ($e' = i = 0$) and for $\sigma = \pi$ a family of unstable fixed points exists that is extended along the resonance and it is associated with strongly chaotic motion that supports the formation of the Hecuba gap. However, for $\sigma = 0$ the corresponding family is stable for eccentricities up to e=0.83 (point U in fig.1a) and, thus, regular orbits should be the dominant feature in this case. Figure 1a shows the main dynamical characteristics for the plane (a, e) at $\sigma = \nu = \sigma_z = 0$. (PB) denotes the family of stable fixed points (pericentric branch) which becomes unstable at the point (U). (S) denotes the main separatrix, originated in the unstable family of fixed points, which separates the plane in two regions. In the central region σ librates while, in the outside region, σ circulates. Secondary resonances, between σ and the argument of pericenter ω (σ/ω), are obtained in the region (R). They are activated in the elliptic or/and in the spatial case producing chaos

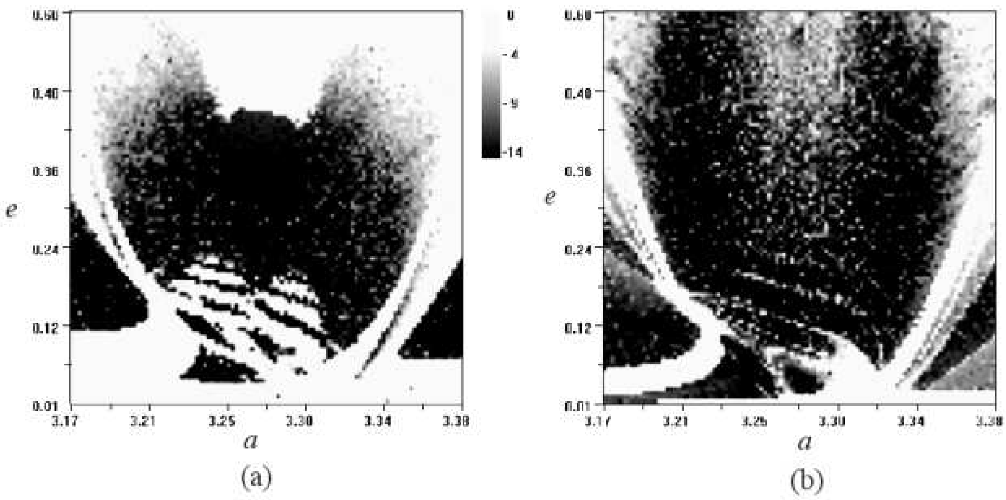

Figure 2: Spectral Maps (a) The elliptic case ($e' = 0.048, i = 0.0$) (b) the spatial circular case ($e' = 0, i = 5^o$)

(see figure 2). (B1) and (B2) are the bifurcation points for the elliptic and the spatial problem respectively. Finally, (S') is an approximation of the lower border of high eccentricity instabilities, which should be generated by the bifurcated unstable orbits in the elliptic and in the spatial case, secular resonances and the Kozai resonance [7].

4 Resonances and chaotic zones

Passing from the circular planar case (figure 1b) to the elliptic-planar case ($e' = 0.048$) we obtain the map of figure 2a. The central region of the 2:1 resonance is still completed with regular orbits. The width of the main separatrix is enlarged providing the possibility of fast diffusion from low to high eccentricities. The effect of secondary resonances is the formation of chaotic zones and stable islands in the low eccentricity domain ($e < 0.25$). Also the effect of the high eccentricity instabilities is very important producing a strong chaotic region for $e > 0.4$. The same picture is obtained also for the spatial circular case, but both the effect of secondary resonances and the high eccentricity instabilities are relatively weak for orbits with low inclination.

When both the effects of the elliptic motion of Jupiter and the inclination of asteroids are taken into account, the high eccentricity instabilities are enlarged (figure 3a). The region of secondary resonances remains almost the same as the planar-elliptic case. However, a new feature ,which is clearer in the finer grids in figures 3c,3d, is obtained. It is the generation of narrow chaotic zones that cross the region of moderate eccentricities. These zones are formed due to resonances between the argument of pericenter (ω) and the longitude of node (Ω) of the asteroid ($R(\omega/\Omega)$). Although these chaotic zones are thin, they are connected with the large chaotic sea and, therefore, a trajectory, which starts inside a resonance can escape in the high eccentricity domain. $R(\omega/\Omega)$ resonances have been observed for inclination values up to 15^o where they are connected with large chaotic regions that exist for high inclinations. The trajectories examined, show almost regular oscillations of the asteroid eccentricity and inclination. This situation may holds for some hundreds Myrs. Afterwards, the inclination starts to increase but the eccentricity is strongly affected, reaching high values ($e > 0.8$), only when inclination becomes greater than 15^o about. Also, we should note that the $R(\omega/\Omega)$ resonances cross the stable islands obtained, by the model used in [7]. Thus the escape of asteroids, through the ω/Ω resonances, is also possible for these regions.

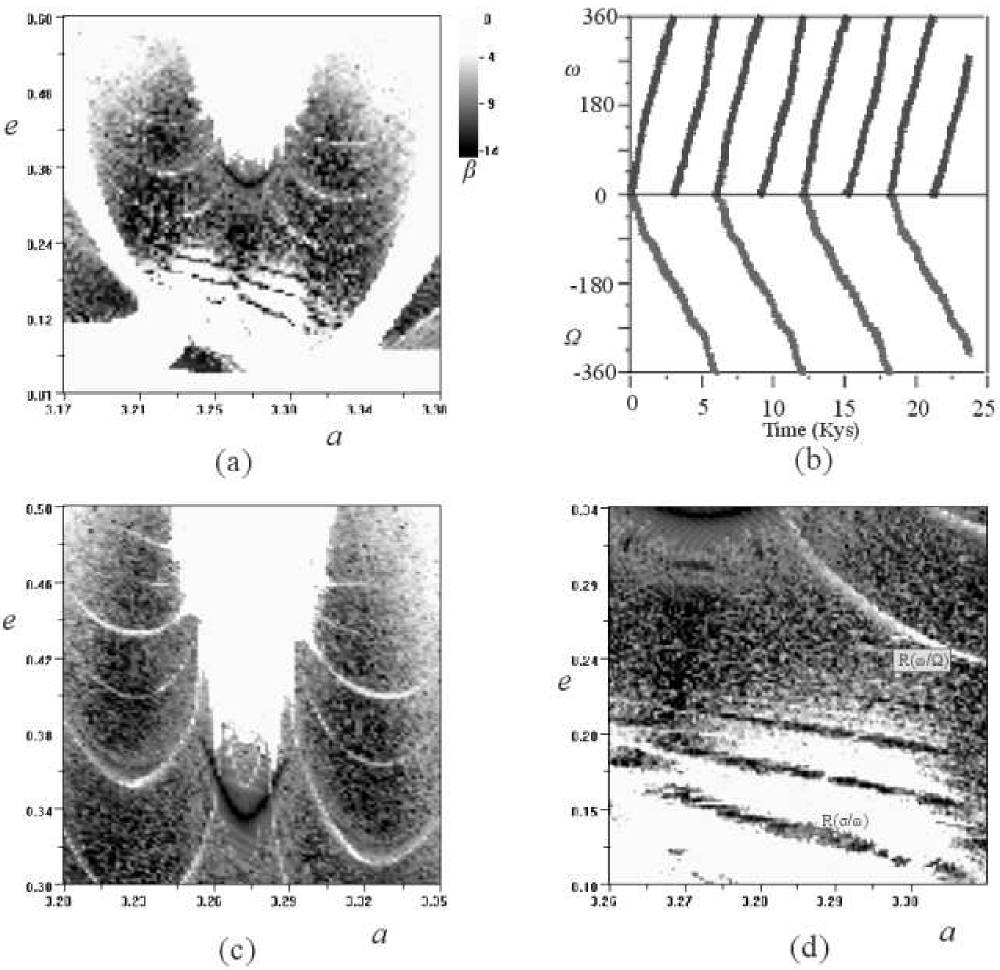

Figure 3: (a) Spectral Map for $e' = 0.048, i = 1^o$ (b) The evolution of ω and Ω in the resonance zone $\omega/\Omega = 2/1$ (c),(d) zoom and finer spectral maps of the map (a)

References

[1] Moons M, 1997, Review of the dynamics in the Kirkwood graps, Cel.Mech. 65, 175-204

[2] Ferraz-Mello, 1999, Slow and fast diffusion in Asteroid-belt resonances:a review , Cel.Mech. 73, 25-37

[3] Sidlichovsky, M. (1992), Mapping For the Asteroidal Resonances, Asron.Astrophys. **259**, 341-348

[4] Hadjidemetriou J, 1996, Symplectic mapping, in Dynamics, Ephemerides and Astrometry in Solar system, Kluwer, Dordrecth (Ferraz-Mello et al eds)

[5] Hadjidemetriou J. and Voyatzis G., 2000, The 2:1 and 3:2 resonant asteroid motion: Asymplectic mapping approach, Cel.Mech. 78, 137-150

[6] Voyatzis, G. and Ichtiaroglou, S. (1992), On the spectral analysis of trajectories in Hamiltonian systems, J.Phys.A:Math. Gen, **25**, 5931-5943.

[7] Moons M, Morbidelli A and Migliorini F., 1998, Dynamical structure of the 2/1 commensurability with Jupiter and the origin of the resonant asteroids.